GEOPHYSICAL RESEARCH LETTERS, VOL. 31, L09207, doi:10.1029/2004GL019453, 2004

On the detection of summertime terrestrial photosynthetic variability from its atmospheric signature

Céline Bonfils
Berkeley Atmospheric Sciences Center, University of California, Berkeley, California, USA

Inez Fung
Berkeley Atmospheric Sciences Center, University of California, Berkeley, California, USA

Scott Doney
Marine Chemistry and Geochemistry, Woods Hole Oceanographic Institution, Woods Hole, Massachusetts, USA

Jasmin John
Berkeley Atmospheric Sciences Center, University of California, Berkeley, California, USA

Received 8 January 2004; revised 24 March 2004; accepted 1 April 2004; published 11 May 2004.

[1] We identify the climatic signatures of the summertime terrestrial photosynthesis variability using a long simulation of pre-industrial climate performed with the NCAR coupled global climate-carbon model. Since plant physiology controls simultaneously CO_2 uptake and surface fluxes of water, changes in photosynthesis are accompanied by changes in numerous climate variables: daily maximum temperature, diurnal temperature range, Bowen ratio, canopy temperature and tropospheric lapse rate. Results show that these climate variables may be used as powerful proxies for photosynthesis activity for subtropical vegetation and for tropical vegetation when photosynthetic variability may be limited by water availability. *INDEX TERMS:* 0315 Atmospheric Composition and Structure: Biosphere/atmosphere interactions; 0322 Atmospheric Composition and Structure: Constituent sources and sinks; 0330 Atmospheric Composition and Structure: Geochemical cycles; 3322 Meteorology and Atmospheric Dynamics: Land/atmosphere interactions. **Citation:** Bonfils, C., I. Fung, S. Doney, and J. John (2004), On the detection of summertime terrestrial photosynthetic variability from its atmospheric signature, *Geophys. Res. Lett.*, *31*, L09207, doi:10.1029/2004GL019453.

1. Introduction

[2] Quantification of the variability of atmosphere-biosphere fluxes of carbon is important for understanding the carbon cycle and its role in climate. In-situ measurements of ecosystem fluxes, as done in the Fluxnet network [*Baldocchi et al.*, 2001], are necessarily sparse and not readily scalable to large regions. Satellite retrievals of net primary productivity (NPP) from normalized difference vegetation index (NDVI) require a biogeochemical model [e.g., *Randerson et al.*, 1997]. In this study, we explore the use of physical climate variables to quantify changes in photosynthesis intensity during the summer season.

[3] Carbon assimilation and exchanges of water and energy are simultaneously regulated by plant physiology and morphology [*Farquhar and Sharkey*, 1982]. Changes in photosynthesis are thus accompanied by changes in evapotranspiration that in turn markedly modify various climate parameters [e.g., *Levis et al.*, 1999; *Sellers et al.*, 1996b]. For instance, in temperate regions, leaf emergence is coincident with an increase in evapotranspiration and with discontinuities in the seasonal evolution of daily maximum temperature (Tmax), relative humidity [*Schwartz*, 1992], and Bowen ratio (BR, ratio of sensible to latent heat fluxes) [*Baldocchi et al.*, 2001]. A decrease in lower-atmospheric lapse rate (LR) is also observed [*Schwartz*, 1992] as evapotranspiration reduces temperature at the surface more than at 850-hPa. Using the land surface model SiB2, *Collatz et al.* [2000] highlighted a change in physiological activity of vegetation associated with climate change could strongly reduce Tmax and diurnal temperature range (DTR, computed as the difference between Tmax and nighttime temperature Tmin). This finding corroborates that the "dip" observed in the seasonal evolution of DTR from spring to fall is related to the growing season [*Durre and Wallace*, 2001; *Schwartz*, 1996]. *Durre et al.* [2000] showed that Tmax shifts towards higher values when the soil gets drier, especially in regions where local water recycling by plants is important.

[4] This study uses outputs from the NCAR global climate-carbon model to quantify the relationship between variability in climate parameters and summertime photosynthesis, so that such relationships may be used to "hindcast" regional to global scale photosynthesis before the satellite period. The best markers are expected to quantify changes in photosynthesis amplitude and to be easily measurable. In this work, photosynthesis responds only to natural climate variability (interannual to decadal variability in temperature or water cycle), paving the groundwork for later studies that will additionally include limitation in nutrients, CO_2 fertilization, and/or greenhouse effects.

2. Model Description

[5] We analyze the spatial and temporal variations in gross primary production (GPP) and various climate parameters from a 200-year simulation of pre-industrial climate performed using the NCAR Community Climate System

0094-8276/04/2004GL019453$05.00

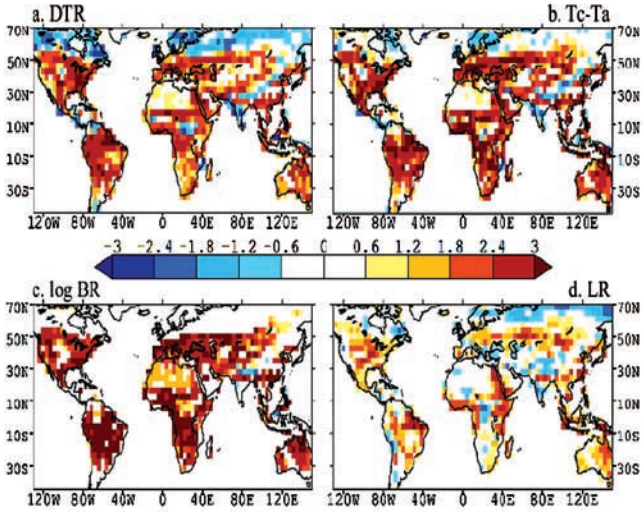

Figure 1. Difference maps of normalized JAS GPP between the lowest 10% and the highest 10% events of (a) DTR (b) Tc-Ta (c) log Bowen ratio and (d) lapse rate.

Model [CCSM1, *Boville and Gent*, 1998]. CCSM1 is composed of an atmospheric general circulation model [CCM3, *Kiehl et al.*, 1998], a land surface scheme [LSM1.1, *Bonan*, 1998], and is forced, in our study, by prescribed climatological sea surface temperatures (SSTs) and sea ice. To the land processes have been added components of the biogeochemical model CASA [*Randerson et al.*, 1997] that describe exchanges and residence times for the different carbon pools in response to environmental conditions. Photosynthesis and evapotranspiration are interactively coupled by the prognostic stomatal conductance parameterization of *Sellers et al.* [1996a]. Phenology is prognostic and the leaf area index (LAI) responds rapidly to GPP and allocation [*Friedlingstein et al.*, 1999]. Leaf mortality is controlled by cold and drought stress [*Dickinson et al.*, 1998].

3. Results and Discussion

3.1. Interannual Variability in Photosynthesis

[6] Atmospheric CO_2 concentration is fixed at 280 ppmv in our simulations, and only the natural variability of photosynthesis and climate is studied. Despite fixed SSTs, the simulation shows a large year-to-year variability of annual GPP (e.g., 12.96 $PgC.y^{-1}$ ±5% in North America north of 22°N), illustrating the large sensitivity of the vegetation activity to the internally generated climate noise. The variability is comparable to the 10% found by *Hicke et al.* [2002] over North America for 1982–1998 using the NDVI.

3.2. Qualitative Markers of Summer GPP

[7] We normalized the anomalies (χ') of a variable (χ) by subtracting the local means and dividing by the local standard deviation from the 200 monthly-averaged values for July–August–September (JAS). For each climate variable, we composited normalized GPP′ for the summers associated with the lowest and the highest 10% events of the normalized climate variable, and calculated the difference in GPP′ between the low and high composites (Figure 1).

[8] Anomalously high photosynthesis, occurring during wet summers (as indicated by β, an index of the relative soil water content weighted by the root density) is accompanied by enhanced transpiration and latent heat loss anomalies. In tropical and temperate regions, this effect is large, and positive GPP′s are accompanied by negative Tmax′ and DTR′. Similarly, high rates of photosynthesis are found when Bowen ratios are unusually small and when tropospheric lapse rates are less steep than normal (in response to increased latent heating of the troposphere). Finally, high GPP′s accompany also a reduction of the gradient between canopy and air temperatures (Tc′-Ta′), since Tc′ is more responsive to surface fluxes and physiological state of vegetation while Ta′ is more affected by air mass circulation.

[9] In addition to re-affirming the control of plant physiology on photosynthesis and land-surface climate, this analysis shows that Tmax′, DTR′, LR′, Tc′-Ta′ and BR′ can constitute good predictors of GPP′, particularly where photosynthesis is sensitive to moisture deficits. It reveals also that the climatic markers of GPP′ are much weaker (BR′) or show an opposite sign (Tmax′, DTR′, Tc′-Ta′, LR′) in monsoon regions where water is not limiting, or in boreal latitudes where cold temperature can limit both photosynthesis and snow melting. In desert areas, GPP is too small to impact near-surface climate. These results are qualitative and we will next investigate how these variables can indicate summertime GPP intensity, where and under which conditions.

3.3. Quantitative Markers of Summer GPP

[10] Table 1 shows regression analyses for various temperate and tropical vegetations. In anticipation of "hindcasting" long-term trends in GPP using climatic markers, all regressions have been calculated using 5-year running averages of JAS anomalies. The correlation coefficient r_1 has been calculated using all summers. For clear-sky summers, in addition to the correlation coefficient r_2 and the regression coefficient m, we calculated for each regression the residual sigma σ_r (computed as the part of total variance that is not explained by the linear regression) and the relative error of prediction ε (computed as the ratio of the residual sigma to the JAS average photosynthesis GPP_a).

3.3.1. Case of a Warm Broadleaved Deciduous Forest

[11] For a warm deciduous forest located in southeastern U.S., the mean JAS GPP_a is 6.26 $gC.m^{-2}.d^{-1}$ with a pentad variability of 0.55 $gC.m^{-2}.d^{-1}$. In spite of the diversity of climate conditions at this location, linear relationships are found between GPP′ and different climate anomalies (Table 1 case 1, Figures 2a and 2b). Because carbon uptake and water loss occur simultaneously, the hydrological variable Bowen ratio is the best correlated with GPP′ ($r_2 = -0.92$) and represents its best predictor ($\varepsilon = 4.4\%$). GPP′ is also well predicted by DTR′ ($r_2 = -0.83$, $\varepsilon = 6.4\%$), Tc′-Ta′ ($r_2 = -0.89$, $\varepsilon = 5.2\%$) and lapse rate ($r_2 = -0.51$, $\varepsilon = 9.9\%$), even though these variables are not directly linked to GPP by the model parameterizations. Correlations with Tc′-Ta′ is larger than with DTR′, since Tc and Ta are contemporaneous, unlike Tmin and Tmax that endure different cloud conditions and depths in the planetary

Table 1. Regressions of 5-year Running Mean JAS Anomalies in GPP Versus Running Mean JAS Anomalies for 5 Climate Variables and 5 Vegetation Types[a]

Vegetation type	Variable	r_1	r_2	m	σ	ε
1. warm broadleaf	Tc-Ta	−0.87	−0.89	−4.61	0.33	5.2
deciduous forest	DTR	−0.78	−0.83	−1.38	0.40	6.4
100–70W;30–45N	Tmax	−0.74	−0.85	−0.79	0.39	6.2
JAS; 2505 samples	logBR	−0.90	−0.92	−4.69	0.27	4.4
GPP_a = 6.260	LR	−0.44	−0.51	−1.73	0.62	9.9
2. warm grassland	Tc-Ta	−0.88	−0.88	−3.06	0.36	11.6
115–95W;20–40N	DTR	−0.75	−0.75	−1.54	0.51	16.5
JAS; 2305 samples	Tmax	−0.77	−0.78	−1.06	0.48	15.5
GPP_a = 3.072	logBR	−0.84	−0.84	−3.65	0.36	11.8
	LR	−0.48	−0.49	−2.20	0.67	21.8
3. savanna	Tc-Ta	−0.78	−0.73	−3.81	0.30	2.6
5–55E;25S-Eq	DTR	−0.49	−0.71	−1.68	0.31	2.7
JFM; 236 samples	Tmax	−0.51	−0.64	−1.61	0.34	2.9
GPP_a = 11.63	logBR	−0.83	−0.88	−4.35	0.21	1.8
	LR	−0.48	−0.55	−2.72	0.37	3.2
4. cool needleleaf	Tc-Ta	−0.55	−0.65	−4.07	0.15	3.5
evergreen forest	DTR	−0.39	−0.53	−0.56	0.17	3.9
150–105W;44–65N	Tmax	−0.34	−0.38	−0.22	0.18	4.3
JAS; 1042 samples	logBR	−0.75	−0.78	−3.45	0.12	2.9
GPP_a = 4.259	LR	−0.05	−0.01	−0.01	0.20	4.6
5. tropical broadleaf	Tc-Ta	−0.79	−0.96	−15.0	0.18	1.4
evergreen forest	DTR	−0.55	−0.71	−3.50	0.45	3.5
0–35E;10S-Eq	Tmax	−0.51	−0.86	−3.36	0.33	2.5
JFM; 149 samples	logBR	−0.77	−0.95	−5.80	0.20	1.6
GPP_a = 12.840	LR	−0.34	−0.83	−4.11	0.36	2.8
6. tropical broadleaf	Tc-Ta	−0.91	−0.93	−16.3	0.22	5.1
evergreen forest	DTR	−0.79	−0.80	−2.16	0.35	8.2
0–35E;10S-Eq	Tmax	−0.71	−0.67	−2.86	0.43	10.0
JAS; 975 samples	logBR	−0.95	−0.96	−5.40	0.17	3.9
GPP_a = 4.275	LR	−0.31	−0.09	−0.61	0.57	13.4

[a]Correlation coefficient (r_2), slope (m), residual σ (σ_r in $gC.m^{-2}.d^{-1}$) and error of prediction (ε in %) are calculated for clear-sky summers (downward solar radiation at the surface to incoming insolation at TOA ratio > 62%) while correlation coefficient (r_1) is calculated using all summers. Region, season of study, number of samples of clear-sky summers and mean GPP over the region (in $gC.m^{-2}.d^{-1}$) are indicated.

boundary layer. Lapse rate is the weakest predictor for GPP′, as large-scale dynamics effects on 850-hPa temperatures remain pronounced.

[12] Results have been presented using clear-sky summers since cloudy conditions can strongly mask the influence of vegetation on surface climate [e.g., *Dai et al.*, 1999] and obfuscate GPP estimates. To better isolate GPP effects on DTR, a subset of summers with similar atmospheric opacities has been selected. This subset also yielded the same linear regression relationship as in Table 1 (not shown). Summers without cloud screening only slightly weakens correlations (r_1 in Table 1), showing a little effect of cloudiness on the regression coefficient in this region.

3.3.2. Other Tropical and Mid-Latitudes Vegetation Types

[13] The above analysis has been extended to other locations and vegetation types. Very similar results are found for warm grassland, African savanna (cases 2 and 3), other warm broadleaved deciduous forests (e.g., in southeastern Asia) and European warm crops that are mainly under dry and clear-sky conditions. Similar results are also established in cool grassland and in cool evergreen forest (case 4), but cloud screening is often necessary to obtain better correlations in those regions. In semi-deserts (not shown), where the carbon sink can only be small, correlations are good (e.g., $r_1 = r_2 = -0.70$ between GPP′ and DTR′) but the errors of prediction are large as changes in photosynthesis are small. In rainforests, the relationship is not well established during the rainy season (JFM in southern African rainforest; case 5) but can be much improved after a severe cloud screening that eliminates more than 90% of samples. We can however estimate GPP′ during the dry season (case 6).

[14] For all regions, soil moisture availability (sustained from wintertime or the rainy season) and its effect on stomatal conductance g_c is the main factor limiting GPP′, even though GPP itself is proportional to LAI and its variability. In the case of the warm deciduous forest for instance (case 1), GPP′ is better correlated with g_c' (r_2 = 0.85) than with LAI′ (r_2 = 0.53).

3.3.3. High Latitudes

[15] At high latitudes, GPP variability is large, mainly because of variations in the length of the growing season (here, GPP′ is better correlated with LAI′ than with g_c'). However, as illustrated in Figure 2 for a deciduous forest (10–40°E, 52–70°N), the responses of Tmax′ and DTR′ to changes in GPP are much weaker than at lower latitudes. Responses of BR′, Tc′-Ta′ and LR′ are similarly weak (not shown). Only GPP′ and Tmax′ are well and positively correlated (r = +0.33) indicating that the dominant factor of GPP variability is not water supply, as at lower latitudes, but temperature. The warming that stimulates GPP largely exceeds the cooling induced by transpiration.

[16] However, under very dry conditions (normalized $\beta' < -2$), stomatal conductance variability dominates photosynthesis and transpiration variability. GPP′ and Tmax′ become slightly negatively correlated, and the negative correlations expected between GPP′ and its markers are slightly improved. Similar results are found for other high latitude biomes (tundra, conifer forests). Nevertheless, because of the difficulties of assessing temperature versus moisture controls, climatic variables cannot be used reliably as proxies of GPP anomalies in these regions.

3.3.4. Observations at Harvard Forest

[17] To test our results, regression analysis has been applied to JAS average GPP and DTR anomalies [*Barford et al.*, 2001], using data from Harvard Forest from 1992 to 1999 [available at ftp://ftp.as.harvard.edu/pub/nigec/HU_Wofsy/hf_data/derived_data]. Figure 3a shows a strong

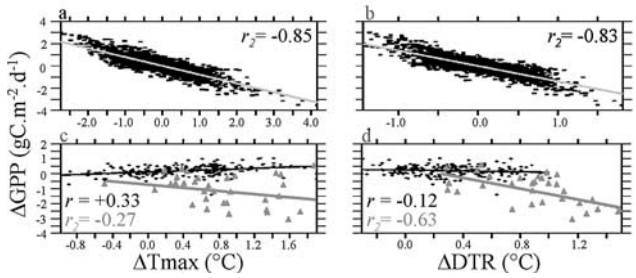

Figure 2. Scatter plots between 5-year running mean JAS anomalies in GPP versus Tmax and GPP versus DTR using clear-sky summers for warm (a–b) and cool (c–d) broadleaved deciduous forests. Regression is calculated for very dry events (gray triangles) selected according to the normalized β ($\beta' < -2$) and for the other events (black, $\beta' > -2$).

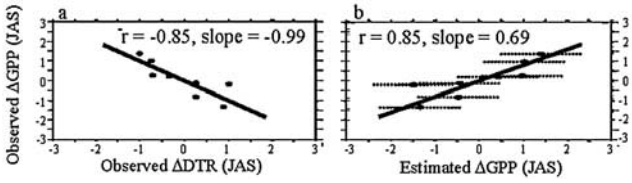

Figure 3. Changes in JAS GPP ($gC.m^{-2}.d^{-1}$) versus (a) changes in JAS DTR (°C) (b) estimated JAS GPP at Harvard Forest from 1992 to 1999.

correlation between GPP′ and DTR′. Using the regression coefficient ($m = -1.42$) and uncertainty ($\sigma_r = 0.9$) obtained from all JAS model outputs (no running mean) for the warm broadleaved forest, we estimate GPP′ as:

$$\Delta GPP_{est} = m.\Delta DTR \pm \sigma_r. \quad (1)$$

[18] Comparison between observed and estimated GPP (Figure 3b) shows that GPP′ can be inferred from the DTR′ in observations. The slope coefficient of 0.69 indicates however that ΔGPP is overestimated. The parameterization of the stomatal conductance is not the only explanation for such differences. Our model includes only natural climate variability and does not take into account the presence and the variations in pollution or volcanic aerosols. The neglect of aerosols, known to strongly reduce observed DTR [*Karl et al.*, 1993] is likely to cause an overestimation of GPP changes.

4. Concluding Remarks

[19] In this study, we highlight five climate variables that are powerful proxies of summertime terrestrial photosynthesis activity at large spatial and/or temporal scales: Tmax, DTR, Tc-Ta, BR and LR. This method works better in tropical and temperate regions where water supply is a limiting factor of GPP and for rainforests during the dry season. At high latitudes, these climate variables cannot be used reliably, since temperature drives GPP rather than responds to its variations.

[20] As a main application, the relationships determined in this study would permit the hindcasting of regional scale GPP variability and trend before 1982, when satellite-derived NPP became available. These proxies can also help constrain our interpretation of the terrestrial carbon sink. For instance, *Schimel et al.* [2001] estimate a contemporary carbon sink in North America of 40 $gC.m^{-2}.y^{-1}$ (0.26 $gC.m^{-2}.d^{-1}$) for the 1990's. According to *Thompson et al.* [1996, equation 9], because of the time delay between GPP and ecosystem respiration, it is possible to sustain such a sink with a linear annual GPP increase of 4 $gC.m^{-2}.y^{-1}$ (0.026 $gC.m^{-2}.d^{-1}$) assuming a carbon turnover time of 20 years and that half of the GPP goes into NPP. Over 10 years, this GPP change could be expressed climatically as (1) a change in the log of the Bowen ratio of −0.06 with an error of ±4.4%; (2) a change in DTR of $-0.19°C \pm 6.4\%$; (3) a change in Tc-Ta of $-0.06°C \pm 5.2\%$; (4) or a change in lapse rate of $-0.15°C.km^{-1} \pm 9.9\%$. The GPP residual variance (σ_r) differs among variables, so that this GPP change may be "detected" with greater confidence using the Bowen ratio ($\sigma_r = 0.27$) than with the lapse rate ($\sigma_r = 0.62$). However, while regional changes in GPP may be more difficult to assess using weather station data of Bowen ratio or Tc-Ta, because they strongly depend on turbulence and stability of the boundary layer, DTR and lapse rate may turn out to have the largest regional footprints. An analysis of the climate proxies could evaluate these hypotheses.

[21] **Acknowledgments.** Support for this work was provided by National Science Foundation grant ATM-9987457, NASA EOS-IDS grant NAG5-9514, WHOI contribution #11077 and the NCAR Climate Simulation Laboratory (CSL). We thank S. Wofsy, S. Urbanski and W. Munger for providing Harvard Forest data. We also thank J. Randerson, A. Angert and S. Biraud and an anonymous reviewer for their helpful comments.

References

Baldocchi, D., et al. (2001), FLUXNET: A new tool to study the temporal and spatial variability of ecosystem-scale carbon dioxide, water vapor, and energy flux densities, *Bull. Am. Meteorol. Soc.*, *82*(11), 2415–2434.

Barford, C. C., S. C. Wofsy, M. L. Goulden, J. W. Munger, E. H. Pyle, S. P. Urbanski, L. Hutyra, S. R. Saleska, D. Fitzjarrald, and K. Moore (2001), Factors controlling long- and short-term sequestration of atmospheric CO2 in a mid-latitude forest, *Science*, *294*(5547), 1688–1691.

Bonan, G. B. (1998), The land surface climatology of the NCAR Land Surface Model coupled to the NCAR Community Climate Model, *J. Clim.*, *11*(6), 1307–1326.

Boville, B. A., and P. R. Gent (1998), The NCAR Climate System Model, version one, *J. Clim.*, *11*(6), 1115–1130.

Collatz, G. J., L. Bounoua, S. O. Los, D. A. Randall, I. Y. Fung, and P. J. Sellers (2000), A mechanism for the influence of vegetation on the response of the diurnal temperature range to changing climate, *Geophys. Res. Lett.*, *27*(20), 3381–3384.

Dai, A., K. E. Trenberth, and T. R. Karl (1999), Effects of clouds, soil moisture, precipitation, and water vapor on diurnal temperature range, *J. Clim.*, *12*(8), 2451–2473.

Dickinson, R. E., M. Shaikh, R. Bryant, and L. Graumlich (1998), Interactive canopies for a climate model, *J. Clim.*, *11*(11), 2823–2836.

Durre, I., and J. M. Wallace (2001), The warm season dip in diurnal temperature range over the eastern United States, *J. Clim.*, *14*(3), 354–360.

Durre, I., J. M. Wallace, and D. P. Lettenmaier (2000), Dependence of extreme daily maximum temperatures on antecedent soil moisture in the contiguous United States during summer, *J. Clim.*, *13*(14), 2641–2651.

Farquhar, G. D., and T. D. Sharkey (1982), Stomatal Conductance and Photosynthesis, *Ann. Rev. Plant Physiol. and Plant Molecul. Biol.*, *33*, 317–345.

Friedlingstein, P., G. Joel, C. B. Field, and I. Y. Fung (1999), Toward an allocation scheme for global terrestrial carbon models, *Global Change Biol.*, *5*(7), 755–770.

Hicke, J. A., G. P. Asner, J. T. Randerson, C. Tucker, S. Los, R. Birdsey, J. C. Jenkins, C. Field, and E. Holland (2002), Satellite-derived increases in net primary productivity across North America, 1982–1998, *Geophys. Res. Lett.*, *29*(10), 1427, doi:10.1029/2001GL013578.

Karl, T. R., P. D. Jones, R. W. Knight, G. Kukla, N. Plummer, V. Razuvayev, K. P. Gallo, J. Lindseay, R. J. Charlson, and T. C. Peterson (1993), A New Perspective on Recent Global Warming - Asymmetric Trends of Daily Maximum and Minimum Temperature, *Bull. Am. Meteorol. Soc.*, *74*(6), 1007–1023.

Kiehl, J. T., J. J. Hack, G. B. Bonan, B. A. Boville, D. L. Williamson, and P. J. Rasch (1998), The National Center for Atmospheric Research Community Climate Model: CCM3, *J. Clim.*, *11*(6), 1131–1149.

Levis, S., J. A. Foley, and D. Pollard (1999), Potential high-latitude vegetation feedbacks on CO_2-induced climate change, *Geophys. Res. Lett.*, *26*(6), 747–750.

Randerson, J. T., M. V. Thompson, T. J. Conway, I. Y. Fung, and C. B. Field (1997), The contribution of terrestrial sources and sinks to trends in the seasonal cycle of atmospheric carbon dioxide, *Global Biogeochem. Cycles*, *11*(4), 535–560.

Schimel, D. S., et al. (2001), Recent patterns and mechanisms of carbon exchange by terrestrial ecosystems, *Nature*, *414*(6860), 169–172.

Schwartz, M. D. (1992), Phenology and Springtime Surface-Layer Change, *Mon. Wea. Rev.*, *120*(11), 2570–2578.

Schwartz, M. D. (1996), Examining the spring discontinuity in daily temperature ranges, *J. Clim.*, *9*(4), 803–808.

Sellers, P. J., D. A. Randall, G. J. Collatz, J. A. Berry, C. B. Field, D. A. Dazlich, C. Zhang, G. D. Collelo, and L. Bounoua (1996a), A revised land surface parameterization (SiB2) for atmospheric GCMs. 1. Model formulation, *J. Clim.*, *9*(4), 676–705.

Sellers, P. J., L. Bounoua, G. J. Collatz, D. A. Randall, D. A. Dazlich, S. O. Los, J. A. Berry, I. Fung, C. J. Tucker, C. B. Field, and T. G. Jensen (1996b), Comparison of radiative and physiological effects of doubled atmospheric CO_2 on climate, *Science*, *271*(5254), 1402–1406.

Thompson, M. V., J. T. Randerson, C. M. Malmstrom, and C. B. Field (1996), Change in net primary production and heterotrophic respiration: How much is necessary to sustain the terrestrial carbon sink?, *Global Biogeochem. Cycles*, *10*(4), 711–726.

C. Bonfils, I. Fung, and J. John, Berkeley Atm. Sci. Center 307 McCone Hall, University of California, Berkeley, CA 94720, USA. (celine@atmos.berkeley.edu)

S. Doney, Marine Chemistry and Geochemistry, Woods Hole Oceanogr. Institution, 360 Wood Hole Rd, Wood Hole, MA 02543, USA.